

A Window Into the Tired Brain: Neurophysiological Dynamics of Visuospatial Working Memory Under Fatigue

Rohith Karthikeyan, Texas A&M University, College Station, Texas, USA,
Joshua Carrizales and Connor Johnson, Texas A&M University, College Station,
Texas, USA, Ranjana K. Mehta , Texas A&M University, College Station, Texas, USA

Objective: We examine the spatiotemporal dynamics of neural activity and its correlates in heart rate and its variability (HR/HRV) during a fatiguing visuospatial working memory task.

Background: The neural and physiological drivers of fatigue are complex, coupled, and poorly understood. Investigations that combine the fidelity of neural indices and the field-readiness of physiological measures can facilitate measurements of fatigue states in operational settings.

Method: Sixteen healthy adults, balanced by sex, completed a 60-minute fatiguing visuospatial working memory task. Changes in task performance, subjective measures of effort and fatigue, cerebral hemodynamics, and HR/HRV were analyzed. Peak brain activation, functional and effective connections within relevant brain networks were contrasted against spectral and temporal features of HR/HRV.

Results: Task performance elicited increased neural activation in regions responsible for maintaining working memory capacity. With the onset of *time-on-task* effects, resource utilization was seen to increase beyond task-relevant networks. Over time, functional connections in the prefrontal cortex were seen to weaken, with changes in the causal relationships between key regions known to drive working memory. HR/HRV indices were seen to closely follow activity in the prefrontal cortex.

Conclusion: This investigation provided a window into the neurophysiological underpinnings of working memory under the *time-on-task* effect. HR/HRV was largely shown to mirror changes in cortical networks responsible for working memory, therefore supporting the possibility of unobtrusive state recognition under ecologically valid conditions.

Applications: Findings here can inform the development of a fieldable index for cognitive fatigue.

Keywords: neuroergonomics, performance, fNIRS, heart rate variability, n-back

Address correspondence to Ranjana K. Mehta, Department of Industrial & Systems Engineering, Texas A&M University, 4020 ETB, College Station, TX 77845, USA. Email: rmehta@tamu.edu

HUMAN FACTORS

Vol. 0, No. 0, ■ ■ ■, pp. 1-16

DOI:10.1177/00187208221094900

Article reuse guidelines: sagepub.com/journals-permissions

Copyright © 2022, Human Factors and Ergonomics Society.

INTRODUCTION

The brain relies on a complex network of resources to facilitate working memory (WM) and associated executive functions (Owen et al., 2005). The ability to sustain attention together with WM capacity remain central components of effective job performance in domains such as emergency response, frontline medical practice, and air-traffic control, where personnel are required to exhibit high levels of comprehension, reasoning, and vigilance for extended periods of time (Causse et al., 2011). In these safety-critical systems, executive functions may be compromised by fatigue due to lapses in work conditions, the workload, hours on the job, or a combination of related factors. Fatigue due to *time-on-task* is known to induce additional cognitive burden, which can impair WM and limit our ability to manage task demands (Möckel et al., 2015). In particular, tasks that afford limited opportunities for individuals to implement compensatory strategies, for example, those with a high workload and a need for sustained attention, are known to be most vulnerable to the effects of fatigue (Matthews & Hancock, 2017). In the laboratory, typical fatigue-WM experiments employ a battery of tests, such as the n-back test (Hopstaken et al., 2015a) the Sternberg task (Persson et al., 2007), the Simon task (Möckel et al., 2015), that provide a performance-oriented measure of the fatigue state experienced by an individual. Indeed, studies have also considered the use of these WM tests as the fatigue induction mechanism by manipulating the *time-on-task* variable (Shigihara et al., 2013). In some cases, even shorter task durations with high workload have elicited an operationally significant fatigue response (Temple et al., 2000). Therefore, there exists a complex

mapping between the workload, motivation, and time, among other factors, that appear to drive the human fatigue response (Matthews & Hancock, 2017).

Different techniques have been proposed to estimate cognitive fatigue including objective indices, and behavioral measures or self-reports (Mehta et al., 2020; Mehta & Agnew, 2015). In the field, there is a need to obtain these measures in an unobtrusive manner, while remaining sensitive to the overall cognitive state changes experienced by the human. Behavioral self-reports are known to be interruptive (O'Donnell, 1986), place additional cognitive demands (Garrison, 2020), and occur at time-scales that lag the fatigue states of the individual (Lohani et al., 2019), at which point intervention may no longer be feasible. Objective indices on the other hand can be prescient and, in some instances, unobtrusive, yet there remain challenges regarding their use in the field (Mehta et al., 2017; Zhu et al., 2017), especially under the constraints of an emergency response setting (Mehta et al., 2020). Therefore, there exists an unfulfilled need for fieldable and proactive fatigue estimation tools in safety-critical field applications. A key requirement to meet this demand is to bridge the gap between the fidelity offered by objective neural indicators and the *fieldability* of physiological indicators and self-reports. The barriers to this goal are primarily mechanistic, given the complex neurophysiological dynamics of *time-on-task* fatigue, working memory, and human attention; and the lack of valid data sets to explore this problem at depth.

Neuroimaging studies have studied the activation of related brain regions during different types of WM tasks (Nee & D'Esposito, 2016; Owens et al., 2018), the relationship between activation and working memory load (Klaassen et al., 2013), and the role of network measures, such as connectivity and causality (Qi et al., 2019; Sala-Llonch et al., 2012), to develop insights around brain function and the neural underpinnings of WM. For example, workload-related activation differences in the prefrontal cortex and changes in effective connectivity (Qi et al., 2019), that is, the influence that one neural system exerts over another (Friston, 2011),

during an n-back WM test using functional near-infrared spectroscopy (fNIRS). The influence of fatigue on WM and its neural correlates have been investigated using similar tools, where studies report the effect of *time-on-task* on executive function using complex network analyses on electroencephalogram (EEG)-based connectivity features and identified the presence of small-world characteristics that were representative of fatigue states (Sun et al., 2014). Other studies have successfully utilized fNIRS based indices to predict workload demands and fatigue correlates when performing ecological valid WM tasks (Dehais et al., 2018). However, translational work that extend these observations to physiological, unobtrusive indicators such as heart rate and its variability (HR/HRV) remain far and few between. In one investigation, researchers found that mental fatigue led to an increase in HR/HRV with *time-on-task*, and counter to their initial hypothesis, found no relationship to motivation-related task engagement in either behavioral or physiological measures during a fatiguing protocol (Gergelyfi et al., 2015). They allude to an exhaustion of neural resources or changes in cognitive control as possible factors that drive this process; however, more evidence is needed to support this hypothesis.

The neurovisceral integration model (NVIM) (Thayer & Lane, 2000) provides a framework to juxtapose vagal activity, prefrontal cortex (PFC) activation, and executive function, one we speculate will help elucidate the ambiguities of earlier findings. Vagal activity can serve as a useful analogue to neural data while relying on unobtrusive sensing instruments. Specifically, the work by Thayer et al. (2009) provides evidence to suggest that the primary role of the PFC during a WM task is toward sensory inhibition, where with increased PFC activity we expect an increase in parasympathetic tone, and therefore an increase in HRV. However, study designs, and associated findings remain variable, with conflicting observations on the relationship between HRV indices and WM demand. For example, in a recent study, authors extended the NVIM to explore comparisons between neural activity and HRV during a response inhibition task (Condy et al., 2020), where they found that

respiratory sinus arrhythmia, a marker of vagal activity was negatively correlated with cerebral oxygenation at baseline—consistent with prior observations from the NVIM (Chang et al., 2013). However, this relationship was seen to deviate from model expectations during active task demands. This reasserts the need for further exploration on task-specificity and environmental demands to assess the relevance of the NVIM framework. Addressing gaps in this space remains critical towards the development of robust state estimation methods free from the practical encumbrances of current neuroimaging tools.

To that end, the present study is centered on understanding WM capacity under the influence of *time-on-task* fatigue using neural and physiological indices. We approach this problem by employing a protracted version of a visuospatial two-back test which demands high WM under constant workload, and sustained attention. The primary aim was to examine the spatiotemporal dynamics of neural activity, and the temporal dynamics of physiological responses during this fatiguing visuospatial WM task. A secondary aim was to compare neurophysiological signal behaviors to expectations from the NVIM framework. Together, fNIRS and HRV based indices may enable advances toward a robust predictive framework for recognizing fatigue-related WM deficits in operational settings.

METHODS

Participants

Sixteen participants were recruited with a mean age of 25.12 ($SD = 3.31$) years. Eight among those participants were female, all from the local student population. For three participants, we had to interrupt the experiment when they needed a break, therefore only 13 among them (seven female) produced unsegmented neural data compatible for subsequent analyses. All participants were self-reported to be right-hand dominant and provided informed consent before the start of the protocol. All procedures were approved by the university's Institutional Review Board and proceeded in accordance with the Ethics Code of the American Psychological Association.

Protocol

On informed consent, participants were equipped with relevant bioinstruments and responded to questionnaires on their background and demographics. Participants were then instructed to rest for 5 minutes with their eyes closed in a seated position to capture a baseline across all sensing instruments. They were then introduced to the visuospatial WM task, which included a training period, followed by the main experiment task. The task consisted of 12 blocks, with each block lasting a duration of 5 minutes. Between blocks, participants responded to single-element questionnaires on their perceived fatigue, effort, and discomfort on a scale of 1–10, with “1” being “low or minimal,” and “10” being “extreme or very high.” The specific phrase for each question was as follows: 1. Please rate the effort you expended in performing this task, 2. Please rate how fatigued you are from performing this task, and 3. Please rate your level of discomfort while performing this task. The time between any two blocks did not exceed 30s. The complete protocol is shown in Figure 1a.

Visuospatial WM task. The experimental task employed in this study was a visuospatial two-back WM, consistent to the one reported in our earlier work (Karthikeyan et al., 2021). The task was presented on a static webpage using a desktop computer, where participants tracked a green circle (diameter = 20 mm) within a 3×3 grid (side = 130 mm), while seated comfortably in front of the screen (diagonal ≈ 600 mm; R240HY 23.8" Wide Screen Monitor, Acer Inc., Taiwan) at a distance of ≈ 500 mm. The circle would appear in different sections of the grid; if the position of the circle matched the one from two steps prior, then the participants would respond with a keypress. The inter-stimulus time was 1000 ms, and the image persistence time was 900 ms. The match probability was set to 0.6, where the interface provided a fixed, temporally randomized number of match events in each block ($N = 94$; see Figure 1b). Before participants began the experiment, they could practice the two-back task under a training mode. The training interface provided feedback on response correctness and response time.

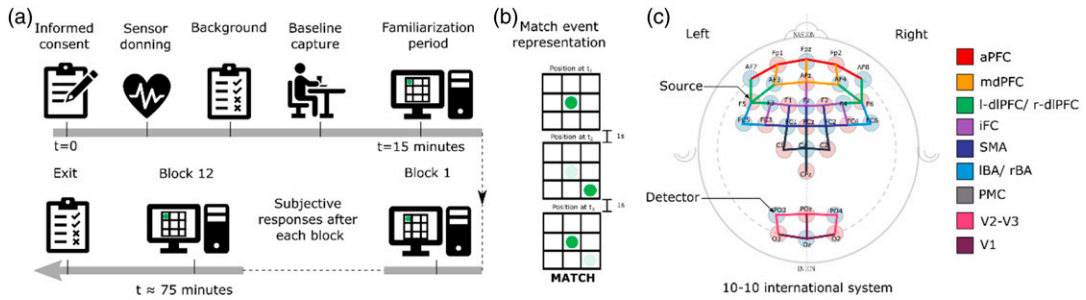


Figure 1. (a) Schematic representation of the experiment protocol. (b) Two-back match event where the user is expected to respond with a keypress. (c) Schematic representation of the probe-map used for neuroimaging via fNIRS. The probe-map consisted of 11 regions of interest derived from the 10–10 EEG system, where the red circles represent infrared (IR) sources, and the blue circles depict the IR detectors.

During the experiment, this feedback was withheld from participants. The interface recorded every keypress or lapse event on the task with time stamps and a response correctness flag (hit, miss or false alarm). For subsequent discussions in this study, the performance measure used was the overall accuracy, which is defined as the ratio of *hits* + *correct omissions* to *hits* + *correct omissions* + *misses* + *false alarms*.

Bioinstruments

Participants were equipped with a head cap that housed sensor and detector probes of a continuous wave functional near-infrared spectroscopy (fNIRS) device (NIRSport2, NIRx Medical Technologies LLC, USA). Cortical hemodynamics was obtained using the fNIRS device at 50 Hz. Near infrared spectra were captured at two wavelengths ($\lambda = 760$ and 850 nm). There was a total of 16 infrared (IR) sources and 16 IR detectors that characterized blood flow in the brain across 46 channels. These channels were originally focused on 11 regions: anterior prefrontal cortex (aPFC), dorsomedial PFC (mdPFC), right dorsolateral PFC (r-dIPFC), left dorsolateral PFC (l-dIPFC), intermediate frontal cortex, right Broca's area, left Broca's area, premotor cortex (PMC), supplementary motor area (SMA), secondary and tertiary visual cortex (V2-V3), and the primary visual cortex (V1; see complete probe-map in Figure 1c). For the statistical investigations and

results reported in this study, we focus on a subset of those regions, namely, l- and r-dIPFC, mdPFC, aPFC, SMA/PMC and the visual cortices (V; aggregating both V1 and V2-V3 regions as one). In addition to the fNIRS device, participants were instrumented with a chest-worn electrocardiography (ECG) device (Actiheart 4, CamNTEch, Inc., UK) that was used to collect ECG data at 128 Hz. Electrodes were placed at the base of the sternum and just beneath the left pectoralis minor muscle.

Signal Preprocessing and Feature Extraction

fNIRS. Light intensity recorded from the fNIRS device was first converted to optical density. The optical density signal was low-pass filtered at 3 Hz to attenuate high frequency noise. Motion artifacts were removed through peak detection and spline interpolation. The smoothed signals were band-pass filtered (0.016–0.5 Hz) to reduce the effect of slow wave drifts and physiological noise in the data (Nuamah et al., 2019). Lastly, the change in oxygenated (ΔHbO), deoxygenated (ΔHbR), and total hemoglobin (ΔHbT) concentration was derived using the modified Beer–Lambert principle using the HOMER2 toolbox (Huppert et al., 2009) on MATLAB. For the scope of the analyses presented in this article we relied on the ΔHbO data which was used to derive region-wise peak activation ($\Delta\text{HbO}_{\text{peak}}$),

functional and effective connectivity measures. The raw time-series ΔHbO was sampled with a window of duration 15 s which accommodates the underlying periodicity of the hemodynamic response (Zhu et al., 2020). The peak values and functional connectivity (FC) measures were derived across each window, after grouping channels based on the relevant regions of interest (ROIs). For FC measures, we relied on Pearson's correlation coefficients that were transformed using Fisher's method (Rhee & Mehta, 2018). Two ROIs were considered functionally connected only when the corresponding Fisher's z -score was ≥ 0.4 (Rubinov & Sporns, 2010).

Time domain effective connectivity (EC) analysis was performed to determine directed causal networks across the ROIs, namely l-dIPFC, r-dIPFC, mdPFC, PMC, SMA, and V regions, using the Multivariate Granger Causality (MVGC) toolbox (Barnett & Seth, 2014). The MVGC, an autoregressive model, is based on the concept of Granger Causality, which posits that a time-series variable A drives another time-series variable B if the time-series history of A along with that of B improves the prediction of B better than its own time-history. For a complete guide to this method of analysis and the use of the MVGC toolbox, see Barnett and Seth (2014). The Granger Causality magnitude was used as a measure of causal strength in our observations. Connections that were found significant were subject to Bonferroni corrections to account for multiple comparisons.

Heart rate variability. The raw ECG signal from the Actiheart was filtered for motion-related artifacts using a multi-resolution threshold (Strasser et al., 2012), and ectopic beats were identified and removed by polynomial interpolation (Marked, 1995). A peak detection algorithm was used to identify R peaks within the ECG signal (Li et al., 1995). The time between successive R peaks, that is, normal-to-normal (NN) interval was then derived from the processed peak signals. We derived five representative statistics for every five-minute window for statistical analysis, three in the time domain (mean heart rate (HR), standard deviation of NN interval (SDNN), and root mean squared of successive differences (RMSSD)), and two in

the frequency domain (low-frequency (0.04–0.15 Hz; LF) and high frequency (0.15–0.4 Hz; HF) power). These features were chosen given their empirical associations with executive function based on the NVIM (Forte et al., 2019). All features were min-max normalized for each participant before statistical analysis (Burr, 2007).

Statistical Analysis

Data partition. The fNIRS data, HR/HRV features, single-element subjective responses, and performance measure were partitioned into five phases—I to V; where the time-series variables were each characterized by their block mean. Each phase consisted of two experiment blocks from phase I to IV, while phase V was made of three blocks. Each block lasted a duration of 5 minutes, with ≈ 30 s of transition time between them, where participants responded to the single-element subjective questionnaires. The last block (no. 12) was dropped from our analyses due to a self-reported anticipatory bias in some participants ($N = 6$).

Analyses. The performance measure (accuracy) was not normally distributed, therefore we relied on the Friedman's test, a non-parametric equivalent to the one-way repeated measures analysis of variance (ANOVA), to assess the main effect of *phase*. Kendall's W (K_w) is reported as an estimate for effect size on the Friedman's test, with Wilcoxon signed rank tests for *post hoc* analyses. On the fNIRS data, a one-way repeated measures ANOVA was applied to assess the main effect of *phase* on peak activation in *each region*, and *between regions* for functional and effectivity connectivity measures. Notably, we relied on aggregated activation data, i.e., mean across related regions, when analyzing changes in functional and effective connectivity. Therefore, while activation was captured across eight regions, only five were used for connectivity analyses for clarity in our visuals and inference (see Figures 2 and 3). On the ANOVA, we report the generalized eta-squared (η^2_g) as a measure of effect size (Bakeman, 2005). All possible pairwise comparisons were made using paired t -tests to assess significance between levels of the within subjects' factor (phase). In

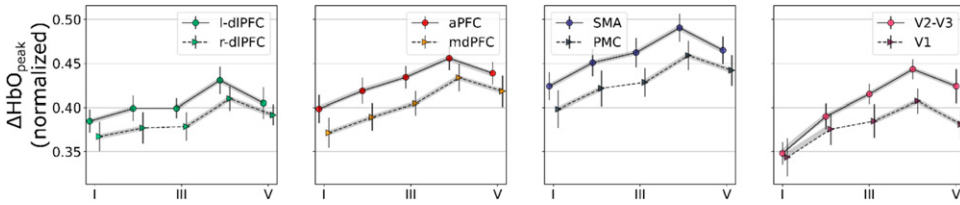


Figure 2. Peak activation across the five phases for each region of interest (ROI). All regions showed a significant main effect of time, shaded segments represent consecutive time points that were significantly different from each other. Error bars represent standard error. The plots are visualized with jitter on the x-axis for clarity of the error bars.

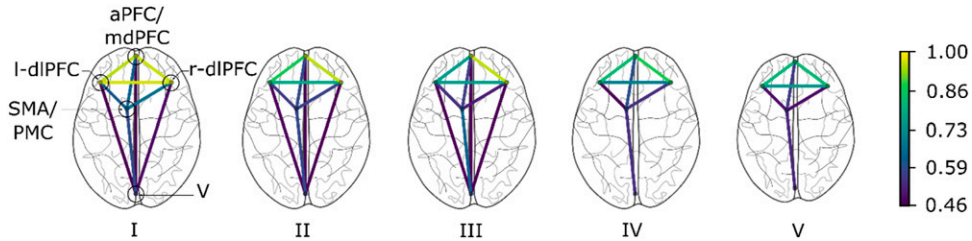


Figure 3. The graphic presents the mean z-score of functional connectivity strength by ROI across all participants at each phase, only those regions with significant connections are represented. *Note.* cranial positions shown here are approximate representations of the regions of interest.

subsequent discussions we primarily rely on comparisons between neighboring phases (i.e., between I–II, II–III, etc.) as highlighted in our plots. Heart rate–based measures were partitioned phase-wise, and subject to a one-way repeated measures ANOVA. Subjective responses were also non-normal, and therefore analyzed using non-parametric tests identical to those employed on the performance data. Bonferroni adjusted p -values were used as a threshold to determine significance where relevant.

RESULTS

Neural Activation

A significant main effect of time was found in peak activation across all brain regions ($F(4, 48) \in [6.82, 17.34]$, all $p < 0.04$, $\eta^2_g \in [0.04–0.26]$). **Figure 2** depicts the peak activation trend across each region. *Post hoc* pairwise comparisons (10 in total for each region) revealed a consistent pattern of differences in the l-dIPFC, r-dIPFC, PMC, and V2-V3 regions, where we observe an increase in peak activation

going from phase I to phases II, III, and IV, respectively ($t(12) \in [-4.47, -3.92]$, all $p < 0.001$); no significant differences were observed between phases II and III (all $p > 0.72$). Peak activation was found to increase further from phase III to IV ($t(12) \in [-3.62, -3.51]$, all $p < 0.0021$), and finally decrease from phase IV to V ($t(12) \in [2.31, 2.59]$, all $p < 0.02$). In the aPFC, mdPFC, SMA, and V2-V3 regions, the increasing trend between peak values of phase I and phases II, III, and IV persisted ($t(12) \in [-2.42, -1.98]$, all $p < 0.036$) with significant increments between each phase until phase IV, and a decrease in activation from phase IV to V, consistent with all other regions ($t(12) \in [-2.72, 2.15]$, all $p < 0.051$).

Functional Connectivity

Figure 3 presents mean z-score of FC across all region-pairs at each time point. In general, we observe that (i) network-wide FC is positive, (ii) a global decrease in FC strength is apparent from phase I to V; and (iii) the number of significant connections was seen to decrease with time.

Table 1 presents the functional connectivity strengths for each region and time point. Here, we aggregated activation data across the visual cortex, that is, V1, V2/V3 channels, the SMA/PMC, and aPFC/mdPFC regions for convenience. A significant effect of time was observed in the connectivity strength across all inter-PFC connections, all PFC—visual cortex (V) connections, and between the SMA/PMC—V regions ($F(4, 48) \in [4.26, 22.34]$, all $p < 0.04$, $\eta^2_g \in [0.14-0.36]$). Connectivity in the PFC, across l-dIPFC, r-dIPFC and aPFC regions, had a mean magnitude of 0.961 in phase I; l-dIPFC and r-dIPFC associations were found to decrease from phase IV-V ($t(12) = 3.61$; $p = 0.0017$); while l-dIPFC—aPFC connections were shown to exhibit marginal recovery through phase III to V

($t(12) \in [-3.74, -3.52]$; all $p < 0.0021$). Connectivity of the PFC with the visual cortices was weak yet significant, and relatively unchanged across phase I–II (all $p > 0.716$); a similar observation was found for connections between the PFC and SMA/PMC regions (all $p > 0.143$). In the terminal stages, that is, phase IV to V, these connections were seen to weaken or were found insignificant.

Effective Connectivity

There was a main effect of time on the effectivity connectivity strengths across a subset of significant networks in this experiment ($F(4, 48) \in [3.42, 26.34]$, all $p < 0.002$, $\eta^2_g \in [0.08, 0.19]$); Figure 4 presents all effective

Table 1. Mean z-scores of functional connectivity in each phase.

Connection	FC _{mean} across each phase				
	I	II	III	IV	V
l-dIPFC–r-dIPFC	0.969±0.088	0.783 ^I ±0.075	0.758±0.085	0.690 ^{III} ±0.088	0.645 ^{IV} ±0.090
l-dIPFC–aPFC	0.951±0.092	0.871 ^I ±0.078	0.758 ^{II} ±0.084	0.833 ^{III} ±0.092	0.821±0.103
l-dIPFC–SMA	0.609±0.083	0.563 ^I ±0.076	0.543±0.080	0.463 ^{III} ±0.078	0.491±0.088
l-dIPFC–V	0.447±0.104	0.474±0.086	0.420±0.089	0.340 ±0.084	0.360±0.098
r-dIPFC–aPFC	0.963±0.088	0.955±0.096	0.957±0.101	0.877 ^{III} ±0.098	0.827 ^{IV} ±0.107
r-dIPFC–SMA	0.666±0.103	0.573 ^I ±0.080	0.514 ^{II} ±0.090	0.543±0.089	0.488 ^{IV} ±0.090
r-dIPFC–V	0.485±0.100	0.455±0.103	0.393±0.102	0.337 ±0.093	0.380±0.099
aPFC–SMA	0.631±0.106	0.585 ^I ±0.086	0.565±0.099	0.594±0.099	0.558±0.105
aPFC–V	0.420±0.106	0.460±0.088	0.395±0.086	0.346 ±0.089	0.352±0.100
SMA–V	0.589±0.121	0.582±0.107	0.629±0.108	0.538 ^{III} ±0.089	0.526±0.102

^aSuperscripts indicate when the mean z-score value of that phase was significantly different than the mean value in the preceding phase, as revealed through post hoc comparisons, with all $p < 0.003$. The shaded cells represent insignificant functional connections (mean z-score < 0.4). Each cell presents the mean value and the standard deviation (M ± SD).

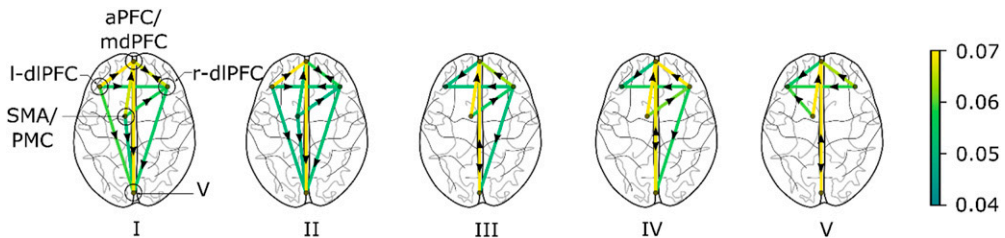


Figure 4. Effective connectivity during the visuospatial working memory task where arrows indicate the direction of causality. Only significant connections are shown. For bi directional connections, the average strength is represented. Note. Cranial positions shown here are approximate representations of the regions of interest.

Table 2. Significant effective connections across the phases of the experiment.

Phase	Connections		Causal strength	
	From	To	F_{mean}	SD
I	aPFC	r-dIPFC ^a	0.064	0.0015
	aPFC	V	0.041	0.0024
	l-dIPFC	aPFC	0.069	0.0021
	l-dIPFC	r-dIPFC	0.051	0.0045
	l-dIPFC	V	0.050	0.0003
	r-dIPFC	aPFC ^a	0.065	0.0005
	r-dIPFC	V	0.048	0.0017
	SMA	aPFC	0.065	0.0041
	SMA	r-dIPFC	0.064	0.0051
	SMA	V	0.046	0.0052
II	aPFC	r-dIPFC ^a	0.053	0.0041
	aPFC	V	0.067	0.0069
	l-dIPFC	aPFC	0.069	0.0013
	l-dIPFC	r-dIPFC ^a	0.050	0.0005
	l-dIPFC	V	0.039	0.0027
	r-dIPFC	l-dIPFC ^a	0.052	0.0048
	r-dIPFC	aPFC ^a	0.051	0.0061
	r-dIPFC	V	0.046	0.0017
	SMA	aPFC	0.046	0.0027
	SMA	r-dIPFC	0.041	0.0023
SMA	V	0.041	0.0052	
III	aPFC	l-dIPFC	0.046	0.0013
	aPFC	V ^a	0.067	0.0082
	r-dIPFC	l-dIPFC	0.049	0.0016
	r-dIPFC	aPFC	0.056	0.0019
	r-dIPFC	V	0.046	0.0024
	SMA	aPFC	0.062	0.0006
	SMA	r-dIPFC	0.052	0.0032
IV	aPFC	l-dIPFC	0.046	0.0022
	aPFC	V ^a	0.063	0.0061
	r-dIPFC	l-dIPFC	0.048	0.0053
	r-dIPFC	aPFC	0.068	0.0012
	r-dIPFC	V	0.046	0.0017
	SMA	aPFC	0.062	0.0042
	SMA	r-dIPFC	0.052	0.0036
	V	aPFC ^a	0.066	0.0092

(Continued)

Table 2. (Continued)

Phase	Connections		Causal strength	
	From	To	F_{mean}	SD
V	aPFC	l-dIPFC	0.054	0.0071
	aPFC	V ^a	0.061	0.0036
	r-dIPFC	l-dIPFC	0.050	0.0022
	r-dIPFC	aPFC	0.061	0.0043
	SMA	aPFC	0.069	0.0061
	SMA	l-dIPFC	0.055	0.0052
	V	aPFC ^a	0.064	0.0027

^amatched superscripts in each phase represent bidirectional connections that were found causally related.

connections deemed significant in each phase using the causal strength metric.

We found unique changes in causal dynamics over time, all significant observations are reported in Table 2, where significance is determined based on the p -values reported by the *mvgc_pval* function in the MVGC toolbox (Barnett & Seth, 2014), the table also reports the mean and standard deviations of the effective connectivity strength. In phase I, we observed unidirectional effective connections originating from the l-dIPFC to the aPFC/mdPFC and r-dIPFC regions (all $p < 0.001$). Significant unidirectional causality was also found between regions in the PFC, SMA/PMC, and the visual cortices (all $p < 0.001$). In phase II, we observed a decrease in F_{mean} compared to those levels seen in phase I ($t(12) \in [1.62, 2.31]$; all $p < 0.03$), along with changes in causal directions, with bidirectional connectivity evidenced between the l-dIPFC-r-dIPFC and aPFC-r-dIPFC regions (all $p < 0.001$). In phase III, connections between the l-dIPFC and visual cortex were not significant (all $p > 0.71$), and the direction of network causality in the PFC was reversed, with aPFC, r-dIPFC regions driving the l-dIPFC (all $p < 0.001$). This change persisted in phase IV, where we also observed bidirectional causal connections between the aPFC—V regions ($p < 0.001$). In the transition from phase IV to V, we

found new causal pathways of significance where the SMA was observed to drive the l-dIPFC ($p < 0.001$), which until phase IV was shown to drive causal networks to the aPFC and r-dIPFC regions (all $p < 0.001$).

Heart Rate Measures

A significant main effect of time was found across all four heart rate–based measures ($F(4, 48) \in [7.71, 14.46]$, all $p < 0.0001$, $\eta^2_g \in [0.08, 0.13]$; Figure 5). In mean HR we observed a significant increase from phase III to IV and IV to V as shown in Figure 3 ($t(12) \in [-3.61, -3.32]$; $p < 0.003$). For the LF measure, *post hoc* comparisons revealed significant differences in the mean values between phase I, and all subsequent phases. Notably, we found that LF-power density increases relative to phase I in all other phases ($t(12) \in [-3.15, -2.79]$; all $p < 0.01$). A similar increase was found going from phase II to III ($t(12) = -2.11$; $p = 0.028$); the measure was found to plateau across phase III–IV ($p = 0.132$), before decreasing across phase IV–V ($t(12) = 3.33$; $p = 0.003$). A significant increase in HF was evident between phase I and II ($t(12) = -2.38$; $p = 0.017$); thereafter HF was seen to remain unaltered across phase II–III ($p = 0.051$) before decreasing from phase III–IV ($t(12) = 2.46$; $p = 0.015$) and plateauing across phase IV–V ($p = 0.76$). In SDNN and RMSSD, we observed significant increases across phase

I–II ($t(12) \in [-3.211, -1.89]$; all $p < 0.041$), and II to III ($t(12) \in [-2.91, -2.23]$; all $p < 0.023$), while a plateau was observed between phase pairs III and IV (all $p > 0.054$), and a decrease in phase IV–V ($t(12) \in [3.55, 3.83]$; all $p < 0.002$).

Performance Accuracy

A main effect of time was found on the performance accuracy metric ($\chi^2_4 = 27.62$, $n = 13$, $p < 0.0001$, $K_w = 0.21$). *Post hoc* analyses revealed a marginal increase in accuracy going from phase I to phase II ($t(12) = -1.91$; $p = 0.041$), a decrease in accuracy from phase III to phase IV ($t(12) = 1.76$; $p = 0.052$), and a further decrease in accuracy levels from phase IV to phase V ($t(12) = 3.33$; $p = 0.003$); see Figure 6a.

Subjective Responses

A main effect of time was found on all three subjective responses, that is, perceived effort, fatigue, and discomfort ($\chi^2_4 \in [47.4, 65.93]$, $n = 13$, all $p < 0.0001$, $K_w \in [0.08, 0.18]$). *Post hoc* comparisons revealed an increase on all three self-reports early in the experiment (phase I–II; $t(12) \in [-2.81, -2.43]$; all $p < 0.016$). This increasing trend persisted through phase III–V for discomfort and fatigue reports ($t(12) \in [-2.73, -2.33]$; all $p < 0.019$); however, effort scores did not vary significantly beyond phase II (all $p > 0.082$); see Figure 6b.

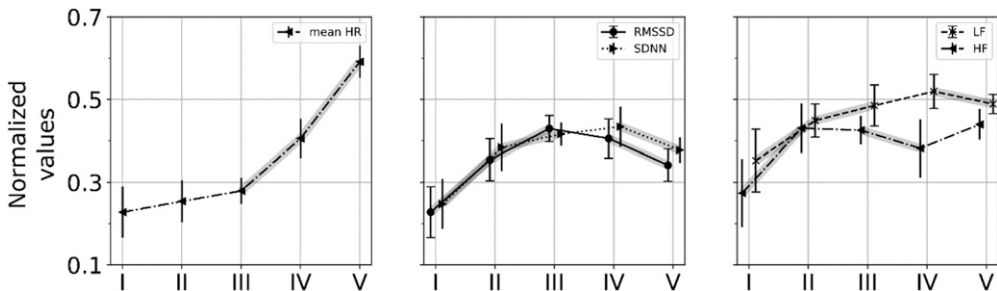


Figure 5. Trends in HR-based measures across the five phases. The plot represents the min-max normalized values for each feature. A significant effect of time was observed across all measures with a small to moderate effect size. Time domain features—Mean HR, RMSSD, and SDNN. Frequency domain features—spectral power densities in the LF (0.04–0.15 Hz) and HF (0.15–0.40 Hz) regimes. Shaded segments represent consecutive time points that were significantly different from each other, error bars represent standard error. The plots are visualized with jitter on the x-axis for clarity of the error bars.

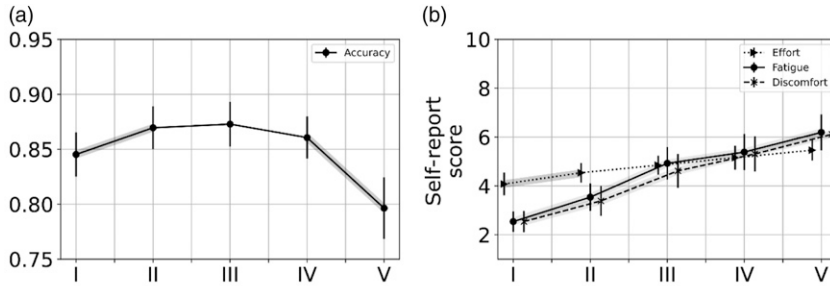


Figure 6. (a) Performance accuracy (%) during the time course of the experiment. (b) Subjective single-element responses on effort, fatigue, and discomfort. Shaded segments represent consecutive time points that were significantly different from each other, error bars represent standard error. The plots are visualized with jitter on the *x*-axis for clarity of the error bars.

DISCUSSION

In this study, we examined the spatiotemporal dynamics of brain activity, and changes in heart rate and its variability (HR/HRV) during a fatiguing visuospatial two-back WM test. In particular, we were interested in the *time-on-task* effect and related deficits during the WM exercise. We know that prolonged cognitive activity at fixed or varying workload levels is known to elicit an increase in both subjective and objective fatigue indices and a decrease in WM performance (Ackerman et al., 2010; Lim et al., 2010); and that this fatigue can manifest as a decrease in accuracy, an increase in self-reported fatigue scores or a decrease in the motivation to continue on task (Krimsky et al., 2017; Möckel et al., 2015). Therefore, we hypothesized that these changes will be evidenced in the present study, driven by a combination of factors underlying the experience of the participant, including, learning during the initial stages of the experiment, a struggle to optimize available neural resources for staying on task, and a decline in the motivation to continue the exercise under the absence of additional rewards.

Our key findings were as follows, participants exhibited a largely unvarying trend in performance accuracy beyond the initial phase, before it worsened through the terminal stages of the experiment. We observed an increase in peak ΔHbO across key regions in the PFC, regions peripheral to the PFC, and the visual cortex until the penultimate experiment phase, where we

note a global decrease in activation levels. These were accompanied by a decline in the number of significant functional associations across brain regions and an increase in perceived fatigue. Finally, the trends in peak activation were mirrored in HR/HRV, where mean HR remained relatively unchanged until phase II before increasing significantly until phase V, while temporal and spectral HRV features were seen to increase till the penultimate phase before diminishing (RMSSD, SDNN) or remaining unaltered (LF, HF—power) through the terminal phase. On the task, we believe a few key processes were at play, early in the experiment (i.e. phase I–II) participants were likely “learning” the task until a stable performance threshold was reached beyond this period, participants expended effort to maintain task performance (III–IV), before they reached a state where they were unable to continue at that level or meet task demands altogether (IV–V).

Some of these observations are clearer when we consider the nature of the task. The visuospatial two-back test demands sustained attention and WM. Although workload on the *N*-back task was not adapted ($N = 2$; constant), in its prolonged format, perceived workload was likely to vary (Grech et al., 2009), therefore eliciting distinct neural and physiological responses associated with the *time-on-task* effect (Dimitrakopoulos et al., 2018), for example, early in the experiment, we believe that the perceived workload is high as participants learn

to perform the task, beyond this period, we anticipate the perceived workload to plateau until *time-on-task* related effects render the task too demanding to continue. There are recognizable brain regions essential to the behavioral adaptation, attentional and response inhibition, and learning characteristic of such WM exercises (D'Esposito et al., 1995), including the prefrontal, motor, and visual cortices (Ahn et al., 2016). However, with time-on-task, we believe that fatigue dominates the behavioral and neurophysiological responses that drive this process (Qi et al., 2019). In our study, we found that participants' self-reports of fatigue increased with time, although their perceived effort remained unaltered beyond phase II. Concomitantly, we observed a significant decline in two-back performance accuracy during the latter half of the experiment. Fatigue is often characterized as the "the reluctance of further effort" (Hopstaken et al., 2015b), and given our observations with the self-reports and in performance outcomes, we reason that the changes seen during this experiment are largely fatigue related.

WM is primarily mediated by networks in the PFC, where domain-specific models postulate that the lateral PFC is functionally organized to process visuospatial information (Barbey et al., 2013). A key component of this network is the l-dIPFC region, which embodies specific computational mechanisms for monitoring and manipulating those representations (Barbey et al., 2013). The primary role of the frontal cortex during such WM tasks is towards attentional inhibition, that is, reducing the influence of distracting streams of information and to retain focus on the task at hand (Engle et al., 1995; Kane & Engle, 2002). Therefore, an increase in PFC activity, early in the experiment, is indicative of the effort employed by the participants in learning the WM task (Petruo et al., 2018). Beyond this period, activation in PFC regions was mostly stable, that is, through phase II-III. One explanation for this is the static workload on the task, which is unlikely to elicit a fatigue response early on (Fan & Smith, 2017). However, beyond phase III, we found that neural activity increased significantly into phase IV, and this was true across all regions, even those

peripheral to the PFC. We reason that this indicates the onset of mental fatigue due to *time-on-task* effects, which prior investigations reveal is preempted by an increase in activation in regions peripheral to those essential for task-related behaviors (Causse et al., 2017). Causse et al., (2017) argue that this is symptomatic of the additional resource demand placed by the need to sustain performance at some threshold, when performance accuracy itself appears to have saturated, further alluding to adaptations arising from fatigue in the form a distributed utilization of cerebral resources.

Brain activation across most of the regions monitored in this study showed an increasing trend, but beyond phase IV, we found a global decrease in activation levels. This is likely due to a fatigue-driven lack of motivation to continue the task, especially in the absence of any additional rewards (Hopstaken et al., 2015a). Our reasoning and inferences around the influence of fatigue and related task disengagement are further supported by our observations with the connectivity data, where we found elevated functional associations in the PFC early during the experiment, when performance was improving with participant learning on the task. Unlike our observations on regional activation, functional connections were seen to largely diminish in strength with time-on-task, with some connections between the prefrontal and visual cortices lost altogether in the later stages of the experiment. These observations are in alignment with prior evidence around the influence of time-on-task induced cognitive fatigue on functional connectivity, where bilateral connections in the PFC and peripheral regions were found to decrease over time (Lim et al., 2010).

The observations in effective connectivity reaffirm the centrality of the lateral PFC in enabling WM performance (Barbey et al., 2013). Early in the task, we found that the l-dIPFC was a prominent driver of connections in the PFC with unidirectional connections to the aPFC and r-dIPFC regions. These regions were also shown to exhibit effective connections with the visual cortices. Over time, however, we observed (i) a role reversal in some of these pathways, with the r-dIPFC, aPFC, and SMA region found to be

driving l-dIPFC activity across phase III–V, (ii) some causal relationships between the prefrontal and visual cortex were lost altogether, and (iii) an overall decrease in network density as a function of time was observed. The reorganization of causal pathways is likely fatigue-driven, with prior investigations reporting topology alterations, disintegrations, and directionality changes driven by fatigue due to *time-on-task* (Wang et al., 2020; Yu et al., 2018; Zhao et al., 2016). While the specific neural mechanisms that originate these changes remain unclear, we hypothesize that this could be an effect of the resource demand placed by sustained task performance, where with time-on-task additional cortical regions are recruited to preserve individual performance at some threshold. This hypothesis is supported by the observation that, beyond phase III, we found the r-dIPFC and APFC regions driving activity in the l-dIPFC region, a pathway that was not previously deemed significant.

Interestingly, the influence of fatigue in our observations was not limited to neural indices. We found distinctive parallels in the response of HR/HRV measures. The neurovisceral integration model (NVIM) posits that the key role of the prefrontal cortex during a WM task is toward attentional inhibition (Thayer et al., 2009). This inhibitory process is reflected in cardiac activity through the control of the *vagus* nerve. In our experiments we expected that this influence would manifest as an increase in heart rate variability (HRV) during the early stages before fatigue-driven declines in the latter parts. The temporal characteristics of HRV, that is, RMSSD and SDNN largely align with this expectation, that is, as PFC activity increased with time-on-task, heart rate variability also increased. Mean HR was largely unchanged early in the experiment (phase I–III), however, beyond this interval, we found a significant increase in mean HR concomitant with a decrease in HRV measures. This fits our expectation of sympathetic dominance or parasympathetic withdrawal under cognitive saturation due to time-on-task (Luque-Casado et al., 2016; Thayer et al., 2009).

Furthermore, in the spectral domain, we found that the LF and HF-power densities mirrored these trends. Under controlled conditions, vagal activity is known to be associated with LF-power (Thayer et al., 2005), and our observations corroborate this idea. The finding in this study that the dynamics of HR/HRV aligned with the NVIM and were seen to reflect changes in neural activity is one that is both interesting and in need of further investigation. In particular, there is need for clarity on the specific processes driving these relationships, for example, lower HR/HRV early on could be driven by learning on the task, before vagally mediated effects or the influence of *time-on-task* fatigue. Nevertheless, we are optimistic that this could be a path forward in our search for robust and prescient state recognition in the field. Especially, knowing that the recognition of WM deficits in emergency responders may benefit from technologies that capture such underlying neurophysiological dynamics unobtrusively.

Limitations of the study are as follows. First, in our experiments we found an anticipation bias in some participants ($N = 6$) during the terminal block, where they returned to an artificial state of alertness, this required that we remove the last block from our analyses to ensure that the true nature of time-on-task related fatigue is preserved. Second, we did not capture motivation or engagement levels during active task performance to minimize disruptions to the participant's experience. However, these measures could have improved how we understand the impact of motivation on fatigue and WM decline, which is shown to offset fatigue states in related experiment (Boksem et al., 2006). Third, besides the task demand, wearing the fNIRS instruments for a prolonged period of time is in itself uncomfortable, which may have skewed participant experiences and self-reports. Fourth, given the duration of the task, vascular nonlinearities may perturb the hemodynamic response signal and therefore our inferences (Huppert, 2016). While we account for issues such as sensor drift and avoid event-related analyses, the effects of vascular

recovery and habituation need careful consideration. Finally, although our end goal is to translate laboratory results into fieldable fatigue detection solutions, our task and setup are not wholly congruent with real-world WM demands; this necessitates ecologically valid experiment paradigms with stakeholders actively engaged in those responsibilities. Nevertheless, our findings support future investigations into the neural and physiological underpinnings that drive WM and related performance decline due to fatigue.

CONCLUSION

Cognitive fatigue can have serious consequences in safety-critical domains such as emergency response. Our study captured fatigue-related neurophysiological dynamics during a 60-minute visuospatial WM task. We found that WM performance was significantly impacted by fatigue-related changes in neural activity. The changes in neural activity, and declines in functional and causal connections, were shown to be temporally coupled with heart rate and its variability. This observation reaffirms the prospect of operationalizing unobtrusive sensing paradigms for recognizing fatigue states in an applied setting. However, larger investigations under ecologically valid conditions are necessary to ensure the generalizability and task-independence of our observations.

KEY POINTS

- On the working memory task, participants invariably reported feeling fatigued and uncomfortable; however, perceived effort did not change.
- Task performance plateaued past the initial phase and was found to decline in the later stages of the experiment.
- An increase in peak brain activation was found in the PFC and in peripheral regions, until the terminal phase, where activation was seen to drop globally.
- Unlike brain activation, connectivity strengths were seen to largely decline with time, and causal connections changed beyond task-relevant regions.

- Trends in peak activation were mirrored in HR/HRV, with temporal and spectral HR/HRV features seen to increase until the penultimate phase.

ACKNOWLEDGMENTS

The work is partially supported by the National Science Foundation under Grant Number 1900704.

ORCID iD

Ranjana K. Mehta  <https://orcid.org/0000-0002-8254-8365>

REFERENCES

- Ackerman, P. L., Kanfer, R., Shapiro, S. W., Newton, S., & Beier, M. E. (2010). Cognitive fatigue during testing: An examination of trait, time-on-task, and strategy influences. *Human Performance, 23*(5), 381–402. <https://doi.org/10.1080/08959285.2010.517720>
- Ahn, S., Nguyen, T., Jang, H., Kim, J. G., & Jun, S. C. (2016). Exploring neuro-physiological correlates of drivers' mental fatigue caused by sleep deprivation using simultaneous EEG, ECG, and fNIRS data. *Frontiers in Human Neuroscience, 10*(848), 219. <https://doi.org/10.3389/fnhum.2016.00219>
- Bakeman, R. (2005). Recommended effect size statistics for repeated measures designs. *Behavior Research Methods, 37*(3), 379–384.
- Barbey, A. K., Koenigs, M., & Grafman, J. (2013). Dorsolateral prefrontal contributions to human working memory. *Cortex, 49*(5), 1195–1205. <https://doi.org/10.1016/j.cortex.2012.05.022>
- Barnett, L., & Seth, A. K. (2014). The MVGC multivariate Granger causality toolbox: A new approach to Granger-causal inference. *Journal of Neuroscience Methods, 223*, 50–68. <https://doi.org/10.1016/j.jneumeth.2013.10.018>
- Boksem, M. A. S., Meijman, T. F., & Lorist, M. M. (2006). Mental fatigue, motivation and action monitoring. *Biological Psychology, 72*(2), 123–132. <https://doi.org/10.1016/j.biopsycho.2005.08.007>
- Burr, R. L. (2007). Interpretation of normalized spectral heart rate variability indices in sleep research: A critical review. *Sleep, 30*(7), 913–919. <https://doi.org/10.1093/sleep/30.7.913>
- Causse, M., Chua, Z., Peysakhovich, V., Del Campo, N., & Matton, N. (2017). Mental workload and neural efficiency quantified in the prefrontal cortex using fNIRS. *Scientific Reports, 7*(1), 5222. <https://doi.org/10.1038/s41598-017-05378-x>
- Causse, M., Dehais, F., & Pastor, J. (2011). Executive functions and pilot characteristics predict flight simulator performance in general aviation pilots. *The International Journal of Aviation Psychology, 21*(3), 217–234. <https://doi.org/10.1080/10508414.2011.582441>
- Chang, C., Metzger, C. D., Glover, G. H., Duyn, J. H., Heinze, H.-J., & Walter, M. (2013). Association between heart rate variability and fluctuations in resting-state functional connectivity. *Neuroimage, 68*, 93–104. <https://doi.org/10.1016/j.neuroimage.2012.11.038>
- Condy, E. E., Friedman, B. H., & Gandjbakche, A. (2020). Probing neurovisceral integration via functional near-infrared

- spectroscopy and heart rate variability. *Frontiers in Neuroscience*, 14, 575589. <https://doi.org/10.3389/fnins.2020.575589>
- D'Esposito, M., Detre, J. A., Alsop, D. C., Shin, R. K., Atlas, S., & Grossman, M. (1995). The neural basis of the central executive system of working memory. *Nature*, 378(6554), 279–281. <https://doi.org/10.1038/378279a0>
- Dehais, F., Dupres, A., Di Flumeri, G., Verdiere, K., Borghini, G., Babiloni, F., & Roy, R. (2018). Monitoring pilot's cognitive fatigue with engagement features in simulated and actual flight conditions using an hybrid fNIRS-EEG passive BCI. In IEEE International Conference on Systems, Man, and Cybernetics (SMC), Miyazaki, Japan, 7–10 October 2018, pp. 544–549.
- Dimitrakopoulos, G. N., Kakkos, I., Dai, Z., Wang, H., Sgarbas, K., Thakor, N., Bezerianos, A., & Sun, Y. (2018). Functional connectivity analysis of mental fatigue reveals different network topological alterations between driving and vigilance tasks. *IEEE Transactions on Neural Systems and Rehabilitation Engineering*, 26(4), 740–749. <https://doi.org/10.1109/TNSRE.2018.2791936>
- Engle, R. W., Conway, A. R., Tuholski, S. W., & Shisler, R. J. (1995). A resource account of inhibition. *Psychological Science*, 6(2), 122–125. <https://doi.org/10.1111/j.1467-9280.1995.tb00318.x>
- Fan, J., & Smith, A. P. (2017). The impact of workload and fatigue on performance. In International Symposium on Human Mental Workload: Models and Applications, Dublin, 28–30 June 2017, pp. 90–105.
- Forte, G., Favieri, F., & Casagrande, M. (2019). Heart rate variability and cognitive function: A systematic review. *Frontiers in Neuroscience*, 13, 710. <https://doi.org/10.3389/fnins.2019.00710>
- Friston, K. J. (2011). Functional and effective connectivity: A review. *Brain Connectivity*, 1(1), 13–36. <https://doi.org/10.1089/brain.2011.0008>
- Garrison, K. E. (2020). *The influence of performance incentives on subjective experiences of mental effort* [PhD thesis, Texas A&M University].
- Gergelyfi, M., Jacob, B., Olivier, E., & Zénon, A. (2015). Dissociation between mental fatigue and motivational state during prolonged mental activity. *Frontiers in Behavioral Neuroscience*, 9, 176. <https://doi.org/10.3389/fnbeh.2015.00176>
- Grech, M. R., Neal, A., Yeo, G., Humphreys, M., & Smith, S. (2009). An examination of the relationship between workload and fatigue within and across consecutive days of work: Is the relationship static or dynamic? *Journal of Occupational Health Psychology*, 14(3), 231–242. <https://doi.org/10.1037/a0014952>
- Hopstaken, J. F., Van Der Linden, D., Bakker, A. B., & Kompier, M. A. J. (2015a). A multifaceted investigation of the link between mental fatigue and task disengagement. *Psychophysiology*, 52(3), 305–315. <https://doi.org/10.1111/psyp.12339>
- Hopstaken, J. F., van der Linden, D., Bakker, A. B., & Kompier, M. A. J. (2015b). The window of my eyes: Task disengagement and mental fatigue covary with pupil dynamics. *Biological Psychology*, 110, 100–106. <https://doi.org/10.1016/j.biopsycho.2015.06.013>
- Huppert, T. J. (2016). Commentary on the statistical properties of noise and its implication on general linear models in functional near-infrared spectroscopy. *Neurophotonics*, 3(1), 010401. <https://doi.org/10.1117/1.NPh.3.1.010401>
- Huppert, T. J., Diamond, S. G., Franceschini, M. A., & Boas, D. A. (2009). HomER: A review of time-series analysis methods for near-infrared spectroscopy of the brain. *Applied Optics*, 48(10), D280–D298. <https://doi.org/10.1364/ao.48.00d280>
- Kane, M. J., & Engle, R. W. (2002). The role of prefrontal cortex in working-memory capacity, executive attention, and general fluid intelligence: An individual-differences perspective. *Psychonomic Bulletin & Review*, 9(4), 637–671. <https://doi.org/10.3758/bf03196323>
- Karthikeyan, R., Smoot, M. R., & Mehta, R. K. (2021). Anodal tDCS augments and preserves working memory beyond time-on-task deficits. *Scientific Reports*, 11(1), 19134. <https://doi.org/10.1038/s41598-021-98636-y>
- Klaassen, E. B., de Groot, R. H. M., Evers, E. A. T., Snel, J., Veerman, E. C. I., Ligtenberg, A. J. M., Jolles, J., & Veltman, D. J. (2013). The effect of caffeine on working memory load-related brain activation in middle-aged males. *Neuropharmacology*, 64, 160–167. <https://doi.org/10.1016/j.neuropharm.2012.06.026>
- Krinsky, M., Forster, D. E., Llabre, M. M., & Jha, A. P. (2017). The influence of time on task on mind wandering and visual working memory. *Cognition*, 169, 84–90. <https://doi.org/10.1016/j.cognition.2017.08.006>
- Lim, J., Wu, W., Wang, J., Detre, J. A., Dinges, D. F., & Rao, H. (2010). Imaging brain fatigue from sustained mental workload: An ASL perfusion study of the time-on-task effect. *Neuroimage*, 49(4), 3426–3435. <https://doi.org/10.1016/j.neuroimage.2009.11.020>
- Li, C., Zheng, C., & Tai, C. (1995). Detection of ECG characteristic points using wavelet transforms. *IEEE Transactions on Biomedical Engineering*, 42(1), 21–28. <https://doi.org/10.1109/10.362922>
- Lohani, M., Payne, B. R., & Strayer, D. L. (2019). A review of psychophysiological measures to assess cognitive states in real-world driving. *Frontiers in Human Neuroscience*, 13, 57. <https://doi.org/10.3389/fnhum.2019.00057>
- Luque-Casado, A., Perales, J. C., Cárdenas, D., & Sanabria, D. (2016). Heart rate variability and cognitive processing: The autonomic response to task demands. *Biological Psychology*, 113, 83–90. <https://doi.org/10.1016/j.biopsycho.2015.11.013>
- Marked, V. (1995). Correction of the heart rate variability signal for ectopics and missing beats. In M. Malik & A. J. Camm (Eds.), *Heart rate variability* (pp. 75–85). Futura. <https://doi.org/10.1016/j.jpl.2017.02.009>
- Matthews, G., & Hancock, P. A. (2017). *The handbook of operator fatigue*. CRC Press.
- Mehta, R. K., & Agnew, M. J. (2015). Subjective evaluation of physical and mental workload interactions across different muscle groups. *Journal of Occupational and Environmental Hygiene*, 12(1), 62–68. <https://doi.org/10.1080/15459624.2014.942455>
- Mehta, R. K., Nuamah, J., Peres, S. C., & Murphy, R. R. (2020). Field methods to quantify emergency responder fatigue: Lessons learned from sUAS deployment at the 2018 Kilauea volcano eruption. *IIEE Transactions on Occupational Ergonomics and Human Factors*, 8(3), 166–174. <https://doi.org/10.1080/24725838.2020.1855272>
- Mehta, R. K., Peres, S. C., Kannan, P., Rhee, J., Shortz, A. E., & Mannan, M. S. (2017). Comparison of objective and subjective operator fatigue assessment methods in offshore shiftwork. *Journal of Loss Prevention in the Process Industries*, 48, 376–381. <https://doi.org/10.1016/j.jlp.2017.02.009>
- Möckel, T., Beste, C., & Wascher, E. (2015). The effects of time on task in response selection—an ERP study of mental fatigue.

- Scientific Reports*, 5(1), 10113. <https://doi.org/10.1038/srep10113>
- Nee, D. E., & D'Esposito, M. (2016). The representational basis of working memory. *Behavioral Neuroscience of Learning and Memory*, 37, 213–230. https://doi.org/10.1007/7854_2016_456
- Nuamah, J. K., Mantooth, W., Karthikeyan, R., Mehta, R. K., & Ryu, S. C. (2019). Neural efficiency of human–robotic feedback modalities under stress differs with gender. *Frontiers in Human Neuroscience*, 13, 287. <https://doi.org/10.3389/fnhum.2019.00287>
- O'Donnell, R. D. (1986). Workload assessment methodology. In K. R. Boff, L. Kaufman, & J. P. Thomas (Eds.), *Handbook of perception and human performance*, Vol. 2. *Cognitive processes and performance* (pp. 1–49). John Wiley & Sons.
- Owen, A. M., McMillan, K. M., Laird, A. R., & Bullmore, E. (2005). N-back working memory paradigm: A meta-analysis of normative functional neuroimaging studies. *Human Brain Mapping*, 25(1), 46–59. <https://doi.org/10.1002/hbm.20131>
- Owens, M. M., Duda, B., Sweet, L. H., & MacKillop, J. (2018). Distinct functional and structural neural underpinnings of working memory. *NeuroImage*, 174, 463–471. <https://doi.org/10.1016/j.neuroimage.2018.03.022>
- Persson, J., Welsh, K. M., Jonides, J., & Reuter-Lorenz, P. A. (2007). Cognitive fatigue of executive processes: Interaction between interference resolution tasks. *Neuropsychologia*, 45(7), 1571–1579. <https://doi.org/10.1016/j.neuropsychologia.2006.12.007>
- Petruo, V. A., Mückschel, M., & Beste, C. (2018). On the role of the prefrontal cortex in fatigue effects on cognitive flexibility - a system neurophysiological approach. *Scientific Reports*, 8(1), 6395. <https://doi.org/10.1038/s41598-018-24834-w>
- Qi, P., Ru, H., Gao, L., Zhang, X., Zhou, T., Tian, Y., Thakor, N., Bezerianos, A., Li, J., & Sun, Y. (2019). Neural mechanisms of mental fatigue revisited: New insights from the brain connectome. *Engineering*, 5(2), 276–286. <https://doi.org/10.1016/j.eng.2018.11.025>
- Rhee, J., & Mehta, R. K. (2018). Functional connectivity during handgrip motor fatigue in older adults is obesity and sex-specific. *Frontiers in Human Neuroscience*, 12, 455. <https://doi.org/10.3389/fnhum.2018.00455>
- Rubinov, M., & Sporns, O. (2010). Complex network measures of brain connectivity: Uses and interpretations. *Neuroimage*, 52(3), 1059–1069. <https://doi.org/10.1016/j.neuroimage.2009.10.003>
- Sala-Llonch, R., Peña-Gómez, C., Arenaza-Urquijo, E. M., Vidal-Piñeiro, D., Bargalló, N., Junqué, C., & Bartrés-Faz, D. (2012). Brain connectivity during resting state and subsequent working memory task predicts behavioural performance. *Cortex*, 48(9), 1187–1196. <https://doi.org/10.1016/j.cortex.2011.07.006>
- Shigihara, Y., Tanaka, M., Ishii, A., Tajima, S., Kanai, E., Funakura, M., & Watanabe, Y. (2013). Two different types of mental fatigue produce different styles of task performance. *Neurology, Psychiatry and Brain Research*, 19(1), 5–11. <https://doi.org/10.1016/j.npbr.2012.07.002>
- Strasser, F., Muma, M., & Zoubir, A. M. (2012). Motion artifact removal in ECG signals using multi-resolution thresholding. Proceedings of the 20th European signal processing conference (EUSIPCO), Bucharest, Romania, 27–31 August 2012, pp. 899–903.
- Sun, Y., Lim, J., Kwok, K., & Bezerianos, A. (2014). Functional cortical connectivity analysis of mental fatigue unmasks hemispheric asymmetry and changes in small-world networks. *Brain and Cognition*, 85C(1), 220–230. <https://doi.org/10.1016/j.bandc.2013.12.011>
- Temple, J. G., Warm, J. S., Dember, W. N., Jones, K. S., LaGrange, C. M., & Matthews, G. (2000). The effects of signal salience and caffeine on performance, workload, and stress in an abbreviated vigilance task. *Human Factors*, 42(2), 183–194. <https://doi.org/10.1518/001872000779656480>
- Thayer, J. F., Hansen, A. L., Saus-Rose, E., & Johnsen, B. H. (2009). Heart rate variability, prefrontal neural function, and cognitive performance: The neurovisceral integration perspective on self-regulation, adaptation, and health. *Annals of Behavioral Medicine*, 37(2), 141–153. <https://doi.org/10.1007/s12160-009-9101-z>
- Thayer, J. F., Hansen, A. L., Sollers, & Johnsen, B. H. (2005 May). Heart rate variability as an index of prefrontal neural function in military settings. In *Biomonitoring for physiological and cognitive performance during military operations* (Vol. 5797, pp. 71–77). International Society for Optics and Photonics.
- Thayer, J. F., & Lane, R. D. (2000). A model of neurovisceral integration in emotion regulation and dysregulation. *Journal of Affective Disorders*, 61(3), 201–216. [https://doi.org/10.1016/S0165-0327\(00\)00338-4](https://doi.org/10.1016/S0165-0327(00)00338-4)
- Wang, H., Liu, X., Hu, H., Wan, F., Li, T., Gao, L., Bezerianos, A., Sun, Y., & Jung, T.-P. (2020). Dynamic reorganization of functional connectivity unmasks fatigue related performance declines in simulated driving. *IEEE Transactions on Neural Systems and Rehabilitation Engineering*, 28(8), 1790–1799. <https://doi.org/10.1109/TNSRE.2020.2999599>
- Yu, S., Bezerianos, A., Thakor, N., & Li, J. (2018). Functional brain network analysis reveals time-on-task related performance decline. In 40th Annual International Conference of the IEEE Engineering in Medicine and Biology Society (EMBC), Honolulu, HI, 18–21 July 2018, pp. 271–274.
- Zhao, C., Zhao, M., Yang, Y., Gao, J., Rao, N., & Lin, P. (2016). The reorganization of human brain networks modulated by driving mental fatigue. *IEEE Journal of Biomedical and Health Informatics*, 21(3), 743–755. <https://doi.org/10.1109/JBHI.2016.2544061>
- Zhu, Y., Jankay, R. R., Pieratt, L. C., & Mehta, R. K. (2017). Wearable sensors and their metrics for measuring comprehensive occupational fatigue: A scoping review. *Proceedings of the Human Factors and Ergonomics Society Annual Meeting*, 61(1), 1041–1045. <https://doi.org/10.1177/1541931213601744>
- Zhu, Y., Rodriguez-Paras, C., Rhee, J., & Mehta, R. K. (2020). Methodological approaches and recommendations for functional near-infrared spectroscopy applications in HF/E research. *Human Factors*, 62(4), 613–642. <https://doi.org/10.1177/0018720819845275>

Rohith Karthikeyan (MS, Mechanical Engineering, Texas A&M University, 2017) is a PhD candidate in the J. Mike Walker '66 Department of Mechanical Engineering at Texas A&M University, and a graduate research assistant in the NeuroErgonomics Laboratory at the Wm. Michael Barnes '64 Department of Industrial and Systems Engineering at Texas A&M University.

Joshua Carrizales (Senior, Biomedical Engineering, Texas A&M University, 2021) is in the Department of Biomedical Engineering at Texas A&M University and

an undergraduate researcher in the NeuroErgonomics Laboratory at the Wm. Michael Barnes '64 Department of Industrial and Systems Engineering at Texas A&M University.

Connor D. Johnson (Senior, Biomedical Engineering, Texas A&M University, 2021) is in the Department of Biomedical Engineering at Texas A&M University and an undergraduate researcher in the NeuroErgonomics Laboratory at the Wm. Michael Barnes '64 Department of Industrial and Systems Engineering at Texas A&M University.

Ranjana K. Mehta (PhD, Industrial and Systems Engineering, Virginia Tech University, 2011), is an Associate Professor in the Wm. Michael Barnes '64 Department of Industrial and Systems Engineering and the J. Mike Walker '66 Department of Mechanical Engineering, director of the NeuroErgonomics Laboratory at Texas A&M University, and graduate faculty in the Texas A&M Institute for Neuroscience.

Date received: May 7, 2021

Date accepted: March 27, 2022